

Flavor-violating Higgs and Z boson decays at a future circular lepton collider

Jernej F. Kamenik^{1,2,*}, Arman Korajac^{1,2,†}, Manuel Szwec^{3,‡}, Michele Tammaro^{1,§} and Jure Zupan^{3,||}

¹*Jožef Stefan Institute, Jamova 39, 1000 Ljubljana, Slovenia*

²*Faculty of Mathematics and Physics, University of Ljubljana, Jadranska 19, 1000 Ljubljana, Slovenia*

³*Department of Physics, University of Cincinnati, Cincinnati, Ohio 45221, USA*

 (Received 17 July 2023; accepted 20 December 2023; published 17 January 2024)

Recent advances in b , c , and s quark tagging coupled with novel statistical analysis techniques will allow future high energy and high statistics electron-positron colliders, such as the FCC-ee, to place phenomenologically relevant bounds on flavor violating Higgs and Z decays to quarks. We assess the FCC-ee reach for $Z/h \rightarrow bs, cu$ decays as a function of jet tagging performance. We also update the standard model (SM) predictions for the corresponding branching ratios, as well as the indirect constraints on the flavor violating Higgs and Z couplings to quarks. Using the type III two Higgs doublet model as an example of beyond the standard model physics, we show that the searches for $h \rightarrow bs, cu$ decays at FCC-ee can probe new parameter space not excluded by indirect searches. We also reinterpret the FCC-ee reach for $Z \rightarrow bs, cu$ in terms of the constraints on models with vectorlike quarks.

DOI: [10.1103/PhysRevD.109.L011301](https://doi.org/10.1103/PhysRevD.109.L011301)

Introduction. Flavor changing neutral currents (FCNCs) are forbidden at tree level in the Standard Model (SM) of particle physics, and are as such ideal to search for effects of beyond the SM (BSM) physics. Most of the FCNC observables are accessible at experiments that are done at relatively low energies, but with large statistics. The list of such observables is very long, and involves both quarks and leptons. The classic examples are $\mathcal{B}(\mu \rightarrow e\gamma)$, $\mu \rightarrow e$ conversion rate, $B_{(s)} - \bar{B}_{(s)}$, or $K - \bar{K}$ mixing, $\mathcal{B}(B_s \rightarrow \mu^+\mu^-)$, and many more (for reviews see, e.g., [1–5]).

The situation is different for high energy FCNC observables, where the list is rather short and almost always involves leptons. Examples are $\mathcal{B}(h \rightarrow \ell\ell')$, $\mathcal{B}(Z \rightarrow \ell\ell')$ and $\sigma(pp \rightarrow \ell\ell')$. The exception to this rule are the decays of top quarks, where $t \rightarrow ch, cg, \dots$, can also be probed in high energy collisions, see, e.g., [6–13].

In this Letter we show that, somewhat surprisingly, the on-shell FCNC decays of the Higgs, $\mathcal{B}(h \rightarrow bs) \equiv \mathcal{B}(h \rightarrow \bar{b}s + b\bar{s})$ and $\mathcal{B}(h \rightarrow cu) \equiv \mathcal{B}(h \rightarrow \bar{c}u + c\bar{u})$, can be added to the list of high energy FCNC observables, since

they can be probed at a phenomenologically interesting level at a future lepton collider, such as the FCC-ee [14]. Over the full running period of FCC-ee, the collider is expected to produce $N_h = 6.7 \times 10^5$ h 's [15] and $N_Z = 5 \times 10^{12}$ Z 's [16,17]. As we show in the following, FCC-ee is projected to have a sensitivity to $\mathcal{B}(h \rightarrow bs)$ and $\mathcal{B}(h \rightarrow cu)$ below the indirect bounds from $B_s - \bar{B}_s$ and $D - \bar{D}$ mixing, cf. Table I, and we expect similar sensitivities to apply also to CEPC [18]. For a recent analysis of the $h \rightarrow bs$ reach at ILC, but using b - and c -taggers, see [19], where the leptonic channel reach is consistent with our results [20]. The main reasons for these significant improvements are: (i) the recent advances in b -, c -, and s -jet tagging, (ii) the analysis technique that we advocate for below, which results in excellent sensitivity to these FCNC transitions, and (iii) the relatively clean environment of e^+e^- collisions. The same approach can also be applied to $\mathcal{B}(Z \rightarrow bs)$ and $\mathcal{B}(Z \rightarrow cu)$, however, the phenomenologically interesting branching ratios are still below the floor set by the systematic uncertainties of taggers.

Accessing flavor violating transitions. An analysis strategy that has been successfully applied to $h \rightarrow c\bar{c}$ decays [41,42], as well as to suppressed $t \rightarrow (s, d)W$ transitions [43,44], is to distribute events into different event types according to how many flavor tagged (and anti-tagged) jets they contain. In particular, the inclusion of information about events with light jets was shown in Ref. [43] to lead to significant improvement in sensitivity to $V_{ts,td}$.

*jernej.kamenik@cern.ch

†arman.korajac@ijs.si

‡szewcml@ucmail.uc.edu

§michele.tammaro@ijs.si

||zupanje@ucmail.uc.edu

Published by the American Physical Society under the terms of the [Creative Commons Attribution 4.0 International license](https://creativecommons.org/licenses/by/4.0/). Further distribution of this work must maintain attribution to the author(s) and the published article's title, journal citation, and DOI. Funded by SCOAP³.

TABLE I. The SM predictions and current experimental upper bounds on hadronic FCNC decays of h and Z , either from direct searches (3rd column) or indirect constraints (4th column), where the indirect bounds on $\mathcal{B}(h \rightarrow qq')$ assume no large cancellations, see main text for details. For details on the SM calculations see Supplemental Material [21] (see also Refs. [22–40] therein).

Decay	SM prediction	Exp. bound	Indir. constr.
$\mathcal{B}(h \rightarrow bs)$	$(8.9 \pm 1.5) \times 10^{-8}$	0.16	2×10^{-3}
$\mathcal{B}(h \rightarrow bd)$	$(3.8 \pm 0.6) \times 10^{-9}$	0.16	10^{-3}
$\mathcal{B}(h \rightarrow cu)$	$(2.7 \pm 0.5) \times 10^{-20}$	0.16	2×10^{-2}
$\mathcal{B}(Z \rightarrow bs)$	$(4.2 \pm 0.7) \times 10^{-8}$	2.9×10^{-3}	6×10^{-8}
$\mathcal{B}(Z \rightarrow bd)$	$(1.8 \pm 0.3) \times 10^{-9}$	2.9×10^{-3}	6×10^{-8}
$\mathcal{B}(Z \rightarrow cu)$	$(1.4 \pm 0.2) \times 10^{-18}$	2.9×10^{-3}	4×10^{-7}

Here, we modify the approach of Ref. [43] and apply it to the case of $h \rightarrow bs, cu$ and $Z \rightarrow bs, cu$ decays. For notational expediency we focus first on just the bs final state, and then extend these results to the analysis of cu decays. In both $h \rightarrow bs$ and $Z \rightarrow bs$ decays there are two jets in the final state; in $e^+e^- \rightarrow hZ(h \rightarrow bs, Z \rightarrow ee, \mu\mu)$ there are also two isolated leptons, while the $e^+e^- \rightarrow Z \rightarrow bs$ events only have two jets. Applying the b - and s -taggers to the two jets, the events are distributed in $(n_b, n_s) \in \{(0, 0), (1, 0), (0, 1), (2, 0), (1, 1), (0, 2)\}$ bins, where $n_{b(s)}$ denotes the number of $b(s)$ -tagged jets in the event. The b - and s -taggers need to be orthogonal to ensure no event populates two different (n_b, n_s) bins and is double-counted [45]. We denote the tagger efficiencies as ϵ_β^b and ϵ_β^s , where $\beta = \{l, s, c, b\}$ denotes the flavor of the initial parton ($l = g$ for h and $l = u, d$ for Z).

The expected number of events in the bin (n_b, n_s) is given by

$$\bar{N}_{(n_b, n_s)} = \sum_f p(n_b, n_s | f, \nu) \bar{N}_f(\nu), \quad (1)$$

where the summation is over the relevant (signal and background) decay channels, $f = \{gg, s\bar{s}, c\bar{c}, b\bar{b}, bs\}$ for the h and $f = \{u\bar{u} + d\bar{d}, s\bar{s}, c\bar{c}, b\bar{b}, bs\}$ for the Z , and ν represents all relevant nuisance parameters. The expected number of events in each decay channel is given by

$$\bar{N}_f = \mathcal{B}(Z/h \rightarrow f) N_{Z/h} \mathcal{A}, \quad (2)$$

where $\mathcal{B}(Z/h \rightarrow f)$ are the corresponding branching fractions, $N_{Z/h}$ are the number of Z and h bosons expected to be produced during the FCC-ee run, while \mathcal{A} is the detector acceptance including reconstruction efficiency, which we assume for simplicity to be the same for all the relevant decay channels.

In writing down Eq. (1) we have neglected the backgrounds: the $\tau^+\tau^-$ for $Z \rightarrow bs$ and the Drell-Yan, WW , ZZ for $h \rightarrow bs$. We expect that the inclusion of these

backgrounds will not qualitatively change our results, since for most part they are small enough to constitute only a subleading effect. Perhaps the most worrisome is the ZZ background for $h \rightarrow bs$. Even this we expect in the actual experimental analysis to be either reduced enough through optimized selection to be ignored (e.g., through use of a multivariate classifier trained on other kinematic observables such as the invariant masses and angular correlations), or alternatively it can, in the proposed analysis strategy, be treated as an appropriate small re-scaling of the predicted \bar{N}_f .

The probability distribution $p(n_b, n_s | f, \nu)$ for a given event to end up in the (n_b, n_s) bin depends on a number of nuisance parameters, $\nu = \{\mathcal{B}(h \rightarrow f), \mathcal{B}(Z \rightarrow f'), \epsilon_\beta^\alpha, N_{Z/h}, \mathcal{A}\}$, which are varied within the uncertainties in the numerical analysis [46]. We build a probabilistic model for $p(n_b, n_s | f, \nu)$, with a graphical representation given in Fig. 1 [49]. The probability $p(n_b, n_s | f, \nu)$ depends on the flavor of the initial $Z/h \rightarrow f$ parton decay, where $f = \{u\bar{u} + d\bar{d}(gg), s\bar{s}, c\bar{c}, b\bar{b}, bs\}$ for $Z(h)$, since the tagging efficiencies ϵ_β^α , $\alpha = b, s$, depend on the flavor of the initial parton.

Experimentally, the value of $\mathcal{B}(Z/h \rightarrow bs)$ would be determined by comparing the measured number of events in each (n_b, n_s) bin, $N_{(n_b, n_s)}$, with the expected value $\bar{N}_{(n_b, n_s)}$. The highest sensitivity to $\mathcal{B}(Z/h \rightarrow bs)$ is expected from the $(n_b, n_s) = (1, 1)$ bin, however, keeping also the $(2, 0)$ and $(0, 2)$ bins increases the overall statistical power. In order to estimate the sensitivity of FCC-ee to $\mathcal{B}(Z/h \rightarrow bs)$, as a proof of concept, we can bypass the need for Monte Carlo simulations and work within the Asimov approximation [50,51], both because of the simplicity of the study and especially due to the high statistics environment. That is, we consider an ideal dataset where the observed number of events equals $N_{(n_b, n_s)}^A = \bar{N}_{(n_b, n_s)}(\mathcal{B}(Z/h \rightarrow bs)_0, \nu = \nu_0)$, that is, it equals to the

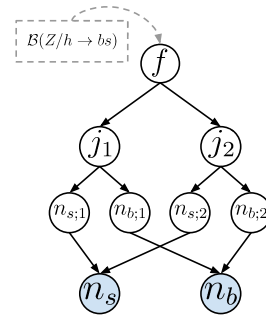


FIG. 1. Graphical representation of the probabilistic model for determining $\mathcal{B}(Z/h \rightarrow bs)$. Starting with the $Z/h \rightarrow f$ partonic decay, where $f = \{u\bar{u} + d\bar{d}(gg), s\bar{s}, c\bar{c}, b\bar{b}, bs\}$ for $Z(h)$, the tagged flavors of the two final state jets, $Z/h \rightarrow j_1 j_2$, are determined by the corresponding s - and b -tagger efficiencies, ϵ_β^α . The arrows denote the probabilities for each event to end up in the (n_b, n_s) bin.

expected number of events for the nominal values of nuisance parameters and the input value of $\mathcal{B}(Z/h \rightarrow bs)_0$. The expected upper bound on $\mathcal{B}(Z/h \rightarrow bs)_0$ is then obtained from a maximum likelihood, allowing nuisance parameters to float [53].

Expected reach at FCC-ee. We first focus on the simplified case where only the b -tagger is used, and obtain the expected exclusion limits on FCNC decays summed over light quark flavors, $\mathcal{B}(h \rightarrow bq) = \mathcal{B}(h \rightarrow bd) + \mathcal{B}(h \rightarrow bs)$. The exclusions are derived from the observed yields in the $n_b = 0, 1, 2$ bins. For simplicity, we parametrize the b -tagger as a function of two parameters: the true positive rate (TPR) ϵ_b^b and the overall effective false positive rate (FPR) for all the other initial parton flavors, ϵ_{gsc}^b .

The expected 95% C.L. upper limits on $\mathcal{B}(h \rightarrow bq)$, assuming only statistical uncertainties, are shown in Fig. 2 (upper). We observe a saturation: for low enough FPR ϵ_{gsc}^b the upper limits become independent of ϵ_{gsc}^b and depend only on ϵ_b^b . With relatively modest TPR $\epsilon_b^b \in [0.4, 0.8]$ and easily achievable FPR $\epsilon_{gsc}^b \lesssim 10^{-2}$ the projected bounds are $\mathcal{B}(h \rightarrow bq) \lesssim (5 - 7) \times 10^{-3}$. This is already

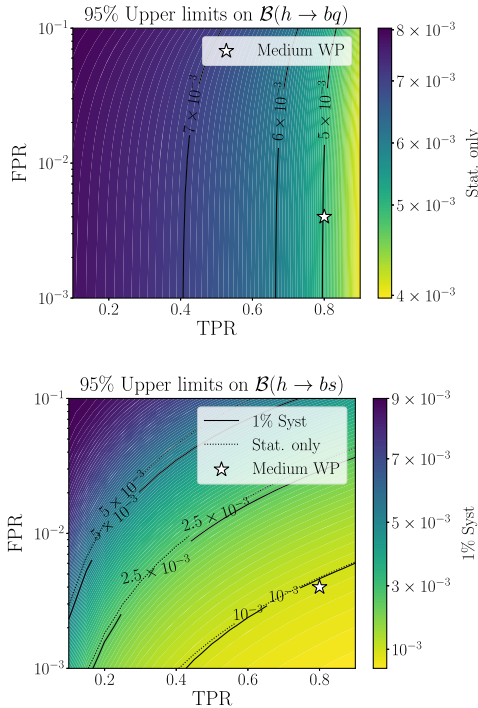


FIG. 2. Upper: expected 95% C.L. upper bounds on $\mathcal{B}(h \rightarrow bq)$ as a function of the b -tagger efficiencies, neglecting systematic uncertainties. Lower: expected 95% C.L. upper bounds on $\mathcal{B}(h \rightarrow bs)$ as a function of TPR and FPR. Solid (dashed) lines and colors are with default (no) systematic uncertainties. The medium working point is based on the taggers introduced in Refs. [55,56]. See main text for details.

in the regime that is interesting for the BSM physics searches, cf. Fig. 4 (upper).

However, the inclusion of strangeness tagging can result in further appreciable improvements in the expected sensitivity. Fig. 2 (lower) shows the expected 95% C.L. bounds on $\mathcal{B}(h \rightarrow bs)$ obtained from the comparison of all possible (n_b, n_s) bins with the predictions. Here, the possible bins are $(n_b, n_s) = \{(0,0), (0,1), (1,0), (1,1), (2,0), (0,2)\}$, where the signal mostly populates the $(n_b, n_s) = (1,1)$ bin, while the remaining bins constrain the backgrounds. To scan over possible tagger efficiencies we assume in Fig. 2 (lower) for the purpose of presentation a common TPR for b - and s -tagging, $\epsilon_b^b = \epsilon_s^s$, and similarly a common FPR, $\epsilon_{lsc}^b = \epsilon_{lsc}^s$. This assumption is not crucial, and is for instance relaxed in the analysis in the Supplemental Material [21]. Nevertheless, we anticipate it to give a reasonable guidance on the expected reach at FCC-ee, if the common FPR is identified as $\text{FPR} = \max(\epsilon_s^b, \epsilon_b^s)$, where $\epsilon_s^b, \epsilon_b^s$ are the actual tagger working point misidentification rates. The reason is that the backgrounds with two misidentified jets are highly suppressed relative to the backgrounds with one misidentified jet, and this is more often than not dominated by the larger misidentification rate. For instance, the performance of the common medium working point (TPR, FPR) = (0.80, 0.004), denoted with a star in Fig. 2 (lower), is very close to the expected 95% upper-limit $\mathcal{B}(h \rightarrow bs) < 9.6 \times 10^{-4}$, obtained when considering all the different efficiencies in the medium working point of the b - and s -taggers introduced in Refs. [55,56], and assuming a 1% systematic uncertainty (the taggers still need to be calibrated). This limit, which does not consider other backgrounds such as Drell-Yan, $WW, ZZ, q\bar{q}$, which we expect to not affect significantly the projected reach, is competitive with indirect measurements and represents a complementary direct probe. We use this as a benchmark expected exclusion in our exploration of the impact on new physics (NP) searches. Note that the SM prediction is orders of magnitude smaller, see Table I, so that any positive signal would mean discovery of NP.

In Fig. 2 (lower) the relative uncertainties on the eight tagger parameters ϵ_β^α are taken to be 1% (the uncertainties are treated as independent, while the central values are common TPR, FPR). The 1% uncertainty is currently below the calibrated scale factors in the LHC analyses [57,58]. However, given the high statistics environment at the FCC-ee, it is reasonable to expect that a dedicated calibration for high precision taggers could reach such relatively low uncertainties. For 1% systematic uncertainties the expected upper bounds on $\mathcal{B}(h \rightarrow bs)$ are statistics limited, except for very large FPR. Incidentally, this also justifies the neglect of systematics in Fig. 2 (upper).

A similar analysis can be performed to arrive at the expected FCC-ee sensitivity to $\mathcal{B}(h \rightarrow cu)$. The main difference is that the sensitivity is determined just by the performance of the c -tagger (there is currently no well

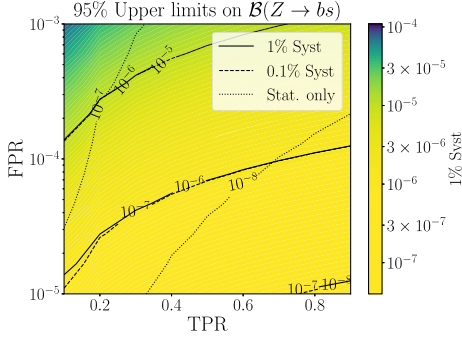


FIG. 3. Expected 95% C.L. upper bound on $\mathcal{B}(Z \rightarrow bs)$ as a function of TPR and FPR. Solid (dashed, dotted) lines and colors are with default 1% (0.1%, no) systematic uncertainties.

established “ u -tagger”). Using the loose (medium) working point for the c -tagger [55,56] leads to the 95% C.L. expected bound for $\mathcal{B}(h \rightarrow cu) < 2.9(2.5) \times 10^{-3}$ [59].

We move next to the case of $Z \rightarrow bs$ decays. As before, we perform a scan over tagger efficiencies, taking the same TPR for b - and s -taggers, $\epsilon_b^b = \epsilon_s^s$, and similarly for the FPR, $\epsilon_{udsc}^b = \epsilon_{udcb}^s$. The resulting expected 95% C.L. upper limits are shown in Fig. 3, where the solid (dashed, dotted) lines correspond to the default 1% (0.1%, no) systematic uncertainties. The FPR of 10^{-4} for ϵ_b^b and few $\times 10^{-3}$ for ϵ_b^s were estimated to be achievable at FCC-ee in Refs. [55,56]. Obtaining the ϵ_b^s well below 10^{-3} level will be hard, since this is roughly the fraction of b -quarks that decay effectively promptly, within the projected vertexing resolution of FCC-ee detectors [61]. To further improve on ϵ_b^s one would thus need to rely on jet shape variables to distinguish between s - and b -jets. For rather optimistic FPR of 10^{-4} the expected reach on $\mathcal{B}(Z \rightarrow bs)$ is $\mathcal{O}(10^{-6})$ [$\mathcal{O}(10^{-7})$] when assuming systematics of 1% (rather aggressive 0.1%), which is still well above the SM value (see Table I). Given existing indirect constraints on effective Zbs couplings coming from $b \rightarrow s\ell^+\ell^-$ transitions, which have already been determined at SM rates, we conclude that it will be challenging to reach bounds on $\mathcal{B}(Z \rightarrow bs)$ that probe parameter space sensitive to NP. Similarly, the expected reach for $Z \rightarrow cu$ is $\mathcal{B}(Z \rightarrow cu) \sim 2 \times 10^{-3}$ [62], and thus well above the sensitivity of indirect probes, e.g., $\mathcal{B}(D^0 \rightarrow \mu^+\mu^-)$. We further quantify these statements below.

Sensitivity to NP. We define the effective FCNC couplings of the h and Z bosons to b and s quarks as

$$\mathcal{L} \supset g_{sb}^L(\bar{s}_L \gamma_\mu b_L)Z^\mu + g_{sb}^R(\bar{s}_R \gamma_\mu b_R)Z^\mu + y_{sb}(\bar{s}_L b_R)h + y_{bs}(\bar{b}_L s_R)h + \text{H.c.}, \quad (3)$$

and similarly for couplings to c and u (or b and d) quarks, with obvious changes in the notation. Equation (3) can be obtained as the effective low energy realization of various extensions of the SM, e.g., the addition of vector-like quarks [19,63], or in the two-Higgs-doublet model

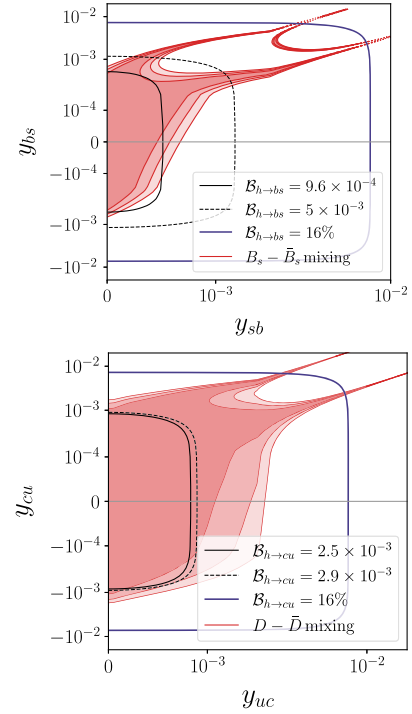


FIG. 4. Upper: current and projected limits on y_{sb} and y_{bs} . Lower: current and projected limits on y_{uc} and y_{cu} . The 1σ , 2σ , 3σ regions are depicted from darker to lighter red.

(2HDM) [64,65]. We provide details on these models in the Supplemental Material [21], while here we focus on the relevant phenomenology.

Existing direct limits on the non-standard hadronic decays of the Z follow from the agreement of the measurement and the SM prediction for the Z hadronic width [66], giving $\mathcal{B}(Z \rightarrow qq') < 2.9 \times 10^{-3}$ at 95% C.L., cf. Table I. Similarly, existing Higgs boson studies at the LHC already impose limits on its undetermined decays $\mathcal{B}(h \rightarrow \text{undet}) < 0.16$ at 95% C.L. [67,68]. Assuming this bound is saturated by $h \rightarrow bs$ or $h \rightarrow cu$ decays, we obtain $|y_{ij}, y_{ji}| \lesssim 7 \times 10^{-3}$, where $ij = \{cu, bs\}$ (shown as purple contours in Fig. 4).

At energies below the h and Z masses, the effective couplings in Eq. (3) give rise to additional contributions in numerous observables, such as the $B_s - \bar{B}_s$ mass splitting and the branching ratio for leptonic decay $B_s \rightarrow \mu^+\mu^-$. Starting from Eq. (3), we perform the matching to the weak effective theory (WET) operators and employ the package WILSON [69] to compute the RGE running down to the scale $\mu \sim m_b$, where we use FLAVIO [70] and SMELLI [71] to compute contributions to the relevant flavor observables and construct the resulting likelihoods.

The $Z - bs$ couplings generate the effective $C_{9,\ell\ell}^{(i)}, C_{10,\ell\ell}^{(i)}$ coefficients in WET. The most stringent constraints on g_{sb}^L, g_{sb}^R therefore come from the $b \rightarrow s\ell^+\ell^-$ transitions. From the global fit we obtain $|g_{sb}^{L,R}| \lesssim 10^{-5}$ with negative values of g_{sb}^L slightly preferred by the current experimental

results [72] (implying $\mathcal{B}(Z \rightarrow bs)$ is essentially constrained to the SM value, within uncertainties). The projected FCC-ee reach, $\mathcal{B}(Z \rightarrow bs) \lesssim 10^{-6}$ (assuming 1% systematics), can probe couplings of $\mathcal{O}(10^{-3})$ and is thus unable to put competitive constraints on NP. The analogous cases of $Z \rightarrow cu, bd$ are discussed in [21] (and Refs. [74–80] therein) with similar conclusions; the indirect bounds $|g_{uc}^{L,R}| \lesssim 3 \times 10^{-4}$ ($|g_{bd}^{L,R}| \lesssim 1 \times 10^{-4}$) imply $\mathcal{B}(Z \rightarrow uc) < 4 \times 10^{-7}$ ($\mathcal{B}(Z \rightarrow bd) < 6 \times 10^{-8}$), which are at least three orders of magnitude below the projected FCC-ee reach.

The situation is very different for $h \rightarrow bs, cu$. The $h - bs$ effective couplings in Eq. (3) generate dominant contributions to scalar $(\bar{b}s)^2$ operators in WET, namely $C_{2,bs}^{(l)}$ and $C_{4,bs}$ [81], which are probed by the B_s meson mixing observables. The resulting bounds on flavor changing couplings read $|y_{bs}, y_{sb}| \lesssim 10^{-3}$ (barring large cancellations), as shown by the red regions in the upper panel in Fig. 4. Similarly, the $D - \bar{D}$ mixing constraints lead to the indirect constraints on $|y_{cu}, y_{uc}| \lesssim \text{few} \times 10^{-3}$, shown in the lower panel in Fig. 4. Excluding the regions with large cancellations, this leads to the approximate indirect bounds on $\mathcal{B}(h \rightarrow q_i q_j)$ quoted in Table I [82]. This is to be compared with the projected upper limits of FCC-ee on $\mathcal{B}(h \rightarrow bs)$ and $\mathcal{B}(h \rightarrow cu)$ shown with black lines in Fig. 4. Taking the medium working point for jet-flavor taggers, the expected reach $\mathcal{B}(h \rightarrow bs) < 9.6 \times 10^{-4}$ translates to the bound $|y_{bs}, y_{sb}| \lesssim 5 \times 10^{-4}$, whereas $\mathcal{B}(h \rightarrow cu) < 2.5 \times 10^{-3}$ translates to $|y_{cu}, y_{uc}| \lesssim 8 \times 10^{-4}$, as shown by the black solid lines. The latter thus improves the strongest indirect constraints on flavor-changing Higgs couplings by a factor of a few. For completeness, we show with lighter lines the expected bounds obtained employing less performative taggers. Details about $h \rightarrow bd$ can be found in [21]), as well as more examples of constraints on 2HDM parameter space away from the limit of light Higgs being the dominant contribution.

Conclusions. The FCC-ee, running at the center of mass energies between the Z boson mass and the $t\bar{t}$ threshold, will allow to measure flavor, electroweak and Higgs processes with an unprecedented level of precision. In this paper we demonstrated the potential of FCC-ee to explore flavor changing decays of the Higgs and Z bosons (with similar expectations for CEPC). The projected sensitivities to $\mathcal{B}(h \rightarrow bs, cu)$, in particular, go well beyond the current constraints from indirect probes, such as the B_s and D meson oscillations. The expected reach does strongly depend on the performance of the flavor taggers, for which we explored a range of achievable efficiencies and uncertainties, based on existing measurements and ongoing studies. Auspiciously, even with rather conservative assumptions, where only the b -tagger is used in the analysis, the projected reach is already such that it will be able to probe significant portions of unconstrained NP parameter space as demonstrated in Fig. 4 (and on the example of a type III 2HDM in [21]). Finally, as a side-result we have also updated the SM predictions for the $h \rightarrow bs, cu$, and $Z \rightarrow bs, cu$ branching ratios. These are orders of magnitude smaller, so that any signal in these channels would unambiguously imply existence of new physics.

Acknowledgments. The authors would like to thank José Zurita for the updated references on the LHC upper limits on nonstandard Higgs boson decays. A.K. thanks Aleks Smolkovič for clarifications regarding FLAVIO. J.Z. and M.S. acknowledge support in part by the DOE Grants No. de-sc0011784 and NSF No. OAC-2103889. J.F.K., A.K., and M.T. acknowledge the financial support from the Slovenian Research Agency (Grant No. J1-3013 and research core funding No. P1-0035). This work was performed in part at the Aspen Center for Physics, which is supported by National Science Foundation Grant No. PHY-2210452.

-
- [1] J. Zupan, Introduction to flavour physics, CERN Yellow Rep. School Proc. **6**, 181 (2019), <https://cds.cern.ch/record/2702255>.
- [2] S. Gori, TASI lectures on flavor physics, *Proc. Sci.*, TASI2018 (2019) 013.
- [3] J. F. Kamenik, Flavour physics and CP violation, in *Proceedings of the 2014 European School of High-Energy Physics* (2016), pp. 79–94, [10.5170/CERN-2016-003.79](https://arxiv.org/abs/10.5170/CERN-2016-003.79).
- [4] W. Altmannshofer and J. Zupan, Snowmass white paper: Flavor model building, in *Snowmass 2021* (2022); [arXiv: 2203.07726](https://arxiv.org/abs/2203.07726).
- [5] Y. Grossman and P. Tanedo, Just a taste: Lectures on flavor physics, in *Theoretical Advanced Study Institute in Elementary Particle Physics: Anticipating the Next Discoveries in Particle Physics* (World Scientific, Singapore, 2018), pp. 109–295, https://doi.org/10.1142/9789813233348_0004.
- [6] J. F. Kamenik, Flavor at low and high p_T , *Proc. Sci.*, Beauty2019 (2020) 046.
- [7] A. Greljo, J. Salko, A. Smolkovič, and P. Stangl, Rare b decays meet high-mass Drell-Yan, *J. High Energy Phys.* **05** (2023) 087.
- [8] J. Fuentes-Martin, A. Greljo, J. Martin Camalich, and J. D. Ruiz-Alvarez, Charm physics confronts high- p_T lepton tails, *J. High Energy Phys.* **11** (2020) 080.
- [9] A. Greljo, J. Martin Camalich, and J. D. Ruiz-Álvarez, Mono- τ signatures at the LHC constrain explanations of B -decay anomalies, *Phys. Rev. Lett.* **122**, 131803 (2019).

- [10] A. Greljo and D. Marzocca, High- p_T dilepton tails and flavor physics, *Eur. Phys. J. C* **77**, 548 (2017).
- [11] D. A. Faroughy, A. Greljo, and J. F. Kamenik, Confronting lepton flavor universality violation in B decays with high- p_T tau lepton searches at LHC, *Phys. Lett. B* **764**, 126 (2017).
- [12] K. Agashe *et al.* (Top Quark Working Group), Working group report: Top quark, in *Snowmass 2013: Snowmass on the Mississippi* (2013); [arXiv:1311.2028](https://arxiv.org/abs/1311.2028).
- [13] M. Cepeda *et al.*, Report from working group 2: Higgs physics at the HL-LHC and HE-LHC, *CERN Yellow Rep. Monogr.* **7**, 221 (2019).
- [14] I. Agapov *et al.*, Future circular lepton collider FCC-ee: Overview and status, in *Snowmass 2021* (2022); [arXiv:2203.08310](https://arxiv.org/abs/2203.08310).
- [15] J. de Blas *et al.*, Higgs boson studies at future particle colliders, *J. High Energy Phys.* **01** (2020) 139.
- [16] M. Mangano *et al.*, FCC physics opportunities: Future circular collider conceptual design report volume 1. Future circular collider, Technical Report No. 6, CERN, Geneva, 2019.
- [17] A. Abada *et al.* (FCC Collaboration), FCC-ee: The lepton collider: Future circular collider conceptual design report volume 2, *Eur. Phys. J. Spec. Top.* **228**, 261 (2019).
- [18] H. Cheng *et al.* (CEPC Physics Study Group), The physics potential of the CEPC. Prepared for the US snowmass community planning exercise (Snowmass 2021), in *Snowmass 2021* (2022); [arXiv:2205.08553](https://arxiv.org/abs/2205.08553).
- [19] D. Barducci and A. J. Helmboldt, Quark flavour-violating Higgs decays at the ILC, *J. High Energy Phys.* **12** (2017) 105.
- [20] Reference [19] also considered the $bj + \text{MET}$ final state where the authors find a slight improvement by going to higher energies, where the relative importance of the Zh contribution decreases, and W -fusion production of the h is the main signal channel. Because the backgrounds are lower, the power of the analysis therefore increases. We focus instead exclusively on the leptonic channel where Zh can be more easily separated from the backgrounds and our Monte-Carlo-free analysis is more trustworthy. We do note that the increase in performance is still qualitatively consistent with our results. A quantitative comparison would require a more detailed study of the systematic uncertainties, which is beyond the scope of present work.
- [21] See Supplemental Material at <http://link.aps.org/supplemental/10.1103/PhysRevD.109.L011301> for further details on the probabilistic model implemented in the analysis of the projected FCC-ee reach; detailed definitions of the relevant statistical estimates implemented in this work; additional results for $h \rightarrow bs$, $h \rightarrow cu$, $Z \rightarrow bs$ and $Z \rightarrow cu$; updated theoretical calculations for the SM FCNC branching ratios and additional details about the two BSM examples.
- [22] L. G. Benitez-Guzmán, I. García-Jiménez, M. A. López-Osorio, E. Martínez-Pascual, and J. J. Toscano, Revisiting the flavor changing neutral current Higgs decays $H \rightarrow q_i q_j$ in the standard model, *J. Phys. G* **42**, 085002 (2015).
- [23] J. I. Aranda, G. González-Estrada, J. Montaña, F. Ramírez-Zavaleta, and E. S. Tututi, Revisiting the rare $H \rightarrow q_i q_j$ decays in the standard model, *J. Phys. G* **47**, 125001 (2020).
- [24] E. Ma and A. Pramudita, Flavor-changing effective neutral-current couplings in the Weinberg-Salam model, *Phys. Rev. D* **22**, 214 (1980).
- [25] M. Clements, C. Footman, A. Kronfeld, S. Narasimhan, and D. Photiadis, Flavor-changing decays of the Z^0 , *Phys. Rev. D* **27**, 570 (1983).
- [26] V. Ganapathi, T. Weiler, E. Laermann, I. Schmitt, and P. M. Zerwas, Flavor-changing z decays: A window to ultraheavy quarks?, *Phys. Rev. D* **27**, 579 (1983).
- [27] L. N. Mihaila, J. Salomon, and M. Steinhauser, Gauge coupling beta functions in the Standard Model to three loops, *Phys. Rev. Lett.* **108**, 151602 (2012).
- [28] K. G. Chetyrkin and M. F. Zoller, Three-loop β -functions for top-Yukawa and the Higgs self-interaction in the standard model, *J. High Energy Phys.* **06** (2012) 033.
- [29] J. Charles, A. Hocker, H. Lacker, S. Laplace, F. R. Le Diberder, J. Malcles, J. Ocariz, M. Pivk, and L. Roos (CKMfitter Group), CP violation and the CKM matrix: Assessing the impact of the asymmetric B factories, *Eur. Phys. J. C* **41**, 1 (2005).
- [30] T. Hahn, Generating Feynman diagrams and amplitudes with FeynArts 3, *Comput. Phys. Commun.* **140**, 418 (2001).
- [31] R. Mertig, M. Bohm, and A. Denner, FEYN CALC: Computer algebraic calculation of Feynman amplitudes, *Comput. Phys. Commun.* **64**, 345 (1991).
- [32] V. Shtabovenko, R. Mertig, and F. Orellana, New developments in FeynCalc 9.0, *Comput. Phys. Commun.* **207**, 432 (2016).
- [33] V. Shtabovenko, R. Mertig, and F. Orellana, FeynCalc 9.3: New features and improvements, *Comput. Phys. Commun.* **256**, 107478 (2020).
- [34] T. Hahn and M. Perez-Victoria, Automatized one loop calculations in four-dimensions and D-dimensions, *Comput. Phys. Commun.* **118**, 153 (1999).
- [35] H. H. Patel, Package-X 2.0: A Mathematica package for the analytic calculation of one-loop integrals, *Comput. Phys. Commun.* **218**, 66 (2017).
- [36] K. G. Chetyrkin and J. H. Kuhn, Mass corrections to the Z decay rate, *Phys. Lett. B* **248**, 359 (1990).
- [37] V. Novikov, L. Okun, A. N. Rozanov, and M. Vysotsky, LEPTOP, [arXiv:hep-ph/9503308](https://arxiv.org/abs/hep-ph/9503308).
- [38] V. A. Novikov, L. B. Okun, A. N. Rozanov, and M. I. Vysotsky, Theory of Z boson decays, *Rep. Prog. Phys.* **62**, 1275 (1999).
- [39] R. L. Workman *et al.* (Particle Data Group), Review of particle physics, *Prog. Theor. Exp. Phys.* **2022**, 083C01 (2022).
- [40] J. R. Andersen *et al.* (LHC Higgs Cross Section Working Group), Handbook of LHC Higgs cross sections: 3. Higgs properties, [10.5170/CERN-2013-004](https://arxiv.org/abs/10.5170/CERN-2013-004) (2013).
- [41] G. Aad *et al.* (ATLAS Collaboration), Direct constraint on the Higgs-charm coupling from a search for Higgs boson decays into charm quarks with the ATLAS detector, *Eur. Phys. J. C* **82**, 717 (2022).
- [42] A. Tumasyan *et al.* (CMS Collaboration), Search for Higgs boson decay to a charm quark-antiquark pair in proton-proton collisions at $s = 13$ TeV, *Phys. Rev. Lett.* **131**, 061801 (2023).

- [43] D. A. Faroughy, J. F. Kamenik, M. Szewc, and J. Zupan, Accessing CKM suppressed top decays at the LHC, [arXiv:2209.01222](https://arxiv.org/abs/2209.01222).
- [44] A. M. Sirunyan *et al.* (CMS Collaboration), Measurement of CKM matrix elements in single top quark t -channel production in proton-proton collisions at $\sqrt{s} = 13$ TeV, *Phys. Lett. B* **808**, 135609 (2020).
- [45] Orthogonality can be achieved with the help of anti-tagging. For example, and as detailed in Ref. [43], an s -tagger can be made orthogonal to a b -tagger simply by combining it with an anti- b -tagger. That is, for a jet to be s -tagged it has to be previously rejected by the b -tagger operating at a looser working point with a higher true and false positive rates than the one used for b -tagging itself.
- [46] The nominal values and uncertainties on the nuisance parameters used in our analysis are listed in the Supplemental Material [21] (see also Refs. [47,48] therein).
- [47] G. Marchiori, Higgs \rightarrow bb/cc/gg/ss with $Z(\ell\ell, \nu\nu)H$ at $\sqrt{s} = 240$ GeV (2023), https://indico.cern.ch/event/1176398/contributions/5208222/attachments/2582981/4456976/2023_01_27%20-%20Higgs%20hadronic%20branching%20ratios%20with%20ZH%20at%20FCCee.pdf.
- [48] R. L. Workman *et al.* (Particle Data Group), Review of particle physics, *Prog. Theor. Exp. Phys.* **2022**, 083C01 (2022).
- [49] The details of the model are relegated to the Supplemental Material [21].
- [50] G. Cowan, K. Cranmer, E. Gross, and O. Vitells, Asymptotic formulae for likelihood-based tests of new physics, *Eur. Phys. J. C* **71**, 1554 (2011); **73**, 2501(E) (2013).
- [51] A recent preliminary analysis which employs Monte Carlo simulations and full tagger kinematic dependency shows similar results, see Ref. [52].
- [52] F. ee Higgs Working Group (FCC Collaboration), Fcc-ee higgs working group, https://indico.cern.ch/event/1304164/contributions/5513419/attachments/2689281/4666483/ZHv_vjj_24072023.pdf.
- [53] See the Supplemental Material [21] (and Ref. [54] contained therein) for further details.
- [54] H. Dembinski, P. Ongmongkolkul, C. Deil, H. Schreiner, M. Feickert, Andrew, C. Burr, J. Watson, F. Rost, A. Pearce, L. Geiger, B. M. Wiedemann, C. Gohlke, Gonzalo, J. Drotleff, J. Eschle, L. Neste, M. E. Gorelli, M. Baak, O. Zapata, and odidev, scikit-hep/iminuit: v2.11.2 (2022), [10.5281/zenodo.6389982](https://zenodo.org/record/6389982).
- [55] F. Bedeschi, L. Gouskos, and M. Selvaggi, Jet flavour tagging for future colliders with fast simulation, *Eur. Phys. J. C* **82**, 646 (2022).
- [56] L. Gouskos, Jet flavor identification for FCCee (2023), <https://indico.cern.ch/event/1176398/contributions/5207197/attachments/2582238/4453976/lg-jettagging-fccee-krakow2023.pdf>.
- [57] A. M. Sirunyan *et al.* (CMS Collaboration), Identification of heavy-flavour jets with the CMS detector in pp collisions at 13 TeV, *J. Instrum.* **13**, P05011 (2018).
- [58] G. Aad *et al.* (ATLAS Collaboration), ATLAS b-jet identification performance and efficiency measurement with $t\bar{t}$ events in pp collisions at $\sqrt{s} = 13$ TeV, *Eur. Phys. J. C* **79**, 970 (2019).
- [59] Further details can be found in the Supplemental Material [21] (see also Ref. [60] therein).
- [60] M. Selvaggi, Higgs Physics at the FCC: Experimental overview (2023), https://indico.cern.ch/event/1278845/contributions/5461471/attachments/2679899/4648628/higgs_physics_exp_pheno.pdf.
- [61] N. Barchetta, P. Collins, and P. Riedler, Tracking and vertex detectors at FCC-ee, *Eur. Phys. J. Plus* **137**, 231 (2022).
- [62] See [21] for further details.
- [63] S. Fajfer, A. Greljo, J. F. Kamenik, and I. Mustac, Light Higgs and vector-like quarks without prejudice, *J. High Energy Phys.* **07** (2013) 155.
- [64] G. C. Branco, P. M. Ferreira, L. Lavoura, M. N. Rebelo, M. Sher, and J. P. Silva, Theory and phenomenology of two-Higgs-doublet models, *Phys. Rep.* **516**, 1 (2012).
- [65] A. Crivellin, A. Kokulu, and C. Greub, Flavor-phenomenology of two-Higgs-doublet models with generic Yukawa structure, *Phys. Rev. D* **87**, 094031 (2013).
- [66] G. Abbiendi *et al.* (OPAL Collaboration), Precise determination of the Z resonance parameters at LEP: 'Zedometry', *Eur. Phys. J. C* **19**, 587 (2001).
- [67] Combined measurements of Higgs boson production and decay using up to 139 fb⁻¹ of proton-proton collision data at $\sqrt{s} = 13$ TeV collected with the ATLAS experiment (2021), <https://cds.cern.ch/record/2789544/>.
- [68] A. Tumasyan *et al.* (CMS Collaboration), A portrait of the Higgs boson by the CMS experiment ten years after the discovery, *Nature (London)* **607**, 60 (2022).
- [69] J. Aebischer, J. Kumar, and D. M. Straub, Wilson: A Python package for the running and matching of Wilson coefficients above and below the electroweak scale, *Eur. Phys. J. C* **78**, 1026 (2018).
- [70] D. M. Straub, flavio: A Python package for flavour and precision phenomenology in the standard model and beyond, [arXiv:1810.08132](https://arxiv.org/abs/1810.08132).
- [71] J. Aebischer, J. Kumar, P. Stangl, and D. M. Straub, A global likelihood for precision constraints and flavour anomalies, *Eur. Phys. J. C* **79**, 509 (2019).
- [72] For details see the Supplemental Material [21] (and Ref. [73] therein).
- [73] M. Algueró, A. Biswas, B. Capdevila, S. Descotes-Genon, J. Matias, and M. Novoa-Brunet, To (b)e or not to (b)e: No electrons at LHCb, *Eur. Phys. J. C* **83**, 648 (2023).
- [74] LHCb Collaboration, Search for rare decays of D^0 mesons into two muons, *Phys. Rev. Lett.* **131**, 041804 (2023).
- [75] M. Petric *et al.* (Belle Collaboration), Search for leptonic decays of D^0 mesons, *Phys. Rev. D* **81**, 091102 (2010).
- [76] M. Ablikim *et al.* (BESIII Collaboration), Search for the decay $D^0 \rightarrow \pi^0 \nu \bar{\nu}$, *Phys. Rev. D* **105**, L071102 (2022).
- [77] R. Bause, M. Golz, G. Hiller, and A. Tayduganov, The new physics reach of null tests with $D \rightarrow \pi \ell \ell$ and $D_s \rightarrow K \ell \ell$ decays, *Eur. Phys. J. C* **80**, 65 (2020); **81**, 219(E) (2021).
- [78] R. Aaij *et al.* (LHCb Collaboration), Search for $D_{(s)}^+ \rightarrow \pi^+ \mu^+ \mu^-$ and $D_{(s)}^+ \rightarrow \pi^- \mu^+ \mu^+$ decays, *Phys. Lett. B* **724**, 203 (2013).
- [79] S. Descotes-Genon, D. A. Faroughy, I. Plakias, and O. Sumensari, Probing lepton flavor violation in meson decays with LHC data, *Eur. Phys. J. C* **83**, 753 (2023).

- [80] L. Allwicher, D. A. Farougy, F. Jaffredo, O. Sumensari, and F. Wilsch, HighPT: A tool for high-pT Drell-Yan tails beyond the standard model, *Comput. Phys. Commun.* **289**, 108749 (2023).
- [81] A. Crivellin, J. Heeck, and D. Müller, Large $h \rightarrow bs$ in generic two-Higgs-doublet models, *Phys. Rev. D* **97**, 035008 (2018).
- [82] We quote present bounds on meson mixing, since no large improvements on such indirect bounds are expected by the FCC-ee era [83].
- [83] J. Charles, S. Descotes-Genon, Z. Ligeti, S. Monteil, M. Papucci, K. Trabelsi, and L. Vale Silva, New physics in B meson mixing: Future sensitivity and limitations, *Phys. Rev. D* **102**, 056023 (2020).